Nanoscale

ROYAL SOCIETY OF CHEMISTRY

PAPER

View Article Online
View Journal | View Issue

Cite this: *Nanoscale*, 2025, **17**, 24035

Nano-biohybrid systems for the targeted delivery of chemotherapeutics

Yi Hsuan Ou,†[a] Wei Heng Chng,†[a] Ram Pravin Kumar Muthuramalingam,†[a] Jeremy Liang,[a,b] Choon Keong Lee,[a] Jia Ning Nicolette Yau[a] and Giorgia Pastorin *[a]

Received 31st May 2025,
Accepted 3rd September 2025

DOI: 10.1039/d5nr02316e

rsc.li/nanoscale

Extracellular vesicles, as a form of cell-derived drug delivery systems (DDSs), have emerged as a novel alternative to their synthetic counterparts (*e.g.* liposomes) due to advantages associated with their intrinsic biocompatibility, non-immunogenicity and tissue-targeting ability. Nonetheless, the clinical application of these naturally secreted vesicles is still hindered by tedious isolation methods, poor drug-loading efficiencies and difficulties in surface functionalization. Our group has conceived a biohybrid DDS, termed nanocell vesicle technology systems (nCVTs), through the fusion of cellular membranes and synthetic lipids. nCVTs are expected to combine the benefits of both the synthetic lipids and the cellular component. Here, we report the production of doxorubicin (DOX)-loaded nCVTs *via* thin-film rehydration and extrusion, showing high loading efficiency, intrinsic targeting abilities, preferential uptake in cancer cells and a superior *in vivo* anticancer effect compared with DOX-loaded liposomes and the free drug. With the administration of DOX-loaded nCVTs, we observed an improvement in tumor growth inhibition without any significant cardiac toxicity detected. Taken together, our results suggest the potential of nCVTs to be developed as a promising DDS for the targeted delivery of chemotherapeutics.

Introduction

Despite tremendous efforts and resources invested to combat cancer, cancer remains one of the leading causes of death worldwide.[1] While traditional chemotherapy is effective in eradicating malignancies by destroying cancer cells, it often lacks specificity and selectivity, resulting in collateral damage to healthy tissues. With advancements in nanotechnology, the use of nanocarriers (*i.e.* carriers at the nanoscale) has offered new opportunities to overcome these limitations. Through the exploitation of the enhanced permeability and retention (EPR) effect, which is a phenomenon resulting from sustained dysregulated angiogenesis in tumors that leads to the formation of leaky tumor vasculature (200–1000 nm), nanocarriers circulating in the bloodstream can extravasate through defective vascular architectures and passively accumulate in tumor tissue.[2] Once extravasated, these nanovesicles need to reach and be internalized by cells at the tumor site.

Several studies have suggested the involvement of cell adhesion molecules (CAMs; *i.e.* ICAM-1, VCAM-1, and E-selectin) and their respective receptors (*i.e.* integrins) in the tumor homing of leukocytes.[3–5] These molecules have been found to play a crucial role in the extravasation of leukocytes (*i.e.* monocytes) into the site of inflammation (including tumors). In addition, inflammatory cytokines, such as tumor necrosis factor-alpha (TNF-α), are known to cause inflamed endothelium (or activated endothelium) to upregulate their expression of CAMs to facilitate the recruitment of leukocytes (*via* receptor–ligand recognition).[6] Furthermore, some cancer cells have also been found to overexpress these CAMs to mediate cancer progression and metastasis.[7–10]

Among the growing number of nanocarriers used as drug delivery systems (DDSs), liposomes, one of the first clinically approved nano-formulations (*i.e.*, liposomal doxorubicin (DOX) Doxil®), can be considered the gold standard in drug delivery.[11,12] Despite the dozens of FDA-approved and clinically used liposomal formulations, challenges such as complement activation and immunogenicity, limited cellular uptake at the diseased area and accelerated blood clearance (ABC) upon repeated administration still remain unresolved.[13] Furthermore, although the addition of polyethylene glycol (PEG) polymeric chains to the liposomal surface ensures prolonged plasma half-life and evades rapid clearance by the reticuloendothelial system (RES)/mononuclear phagocyte system

[a]*Department of Pharmacy and Pharmaceutical Sciences, National University of Singapore, 4 Science Drive 2, Block S9#15, Singapore 117544, Singapore. E-mail: phapg@nus.edu.sg*
[b]*Department of Chemistry and Chemical Biology, Harvard University, Cambridge, MA, USA*
† Equal contribution.

(MPS), numerous recent studies have shown that these PEGylated (stealth) liposomes are plagued with reduced uptake by the target cells and ABC phenomena due to the generation of anti-PEG antibodies.[14,15]

On the contrary, the use of cell-derived DDSs, including drug-loaded extracellular vesicles (EVs), has recently gained traction as one of the promising alternatives to synthetic DDSs. By exploiting the body's natural defences or processes, these cell-derived DDSs increase the extent and specificity of cellular uptake without the need for surface modifications, simply by selecting the type of cells as the starting material. For example, cell-derived DDSs from immune cells like monocytes are expected to display homing abilities towards cancer cells similar to those of their parent cells.[16,17] Despite these favourable properties, most of the cell-derived DDSs are still inferior to conventional systems like liposomes in terms of isolation methods, sample uniformity, drug-loading efficiencies and ease of functionalization for various applications.[18]

Our group recently developed novel liposome-cell biohybrids, termed nano-cell vesicle technology systems (nCVTs), as a means to combine the advantages of both systems.[19,20] nCVTs are formed through the fusion of synthetic lipids with cell membrane components. As a hybrid system, nCVTs are expected to harness the benefits of both synthetic and cell-derived DDS: a relatively simple production method and high drug-loading capability from liposomes, along with the efficient cellular uptake and intrinsic targeting ability inherited from cell-derived DDSs. Specifically, by acquiring specific counter receptors of these CAM molecules (*i.e.* integrins), such as lymphocyte function-associated antigen-1 (LFA-1) from monocytes, nCVTs are expected to harbour targeting abilities towards cells expressing CAMs. We investigated this interaction using TNF-α-treated human umbilical vein endothelial cells (HUVECs), as TNF-α treatment has been reported to significantly upregulate the expression of ICAM-1, VCAM-1, and E-selectin on HUVECs,[21,22] and we proved the important role of nCVTs in targeting inflammatory tumor sites.

In addition, nCVTs may also help alleviate the problem of protein absorption. Protein adsorption (or the formation of a protein corona *in vivo* within minutes of intravenous injection of nanocarriers) is known to impede the targeting and uptake of synthetic nanoparticles.[23] Incorporating cellular components into a hybrid DDS has been reported to alleviate this problem.[24] The "protein corona" is formed by the ungoverned adsorption of biomolecules onto a nanoparticle with high surface energy. While the exact mechanism is still under investigation, here, we demonstrated the effect of the presence of serum on the uptake of nCVTs and liposomes. This would serve as a simple demonstration of how the incorporation of cellular components into nCVTs enables the preservation of their fast and efficient cellular uptake.

In this study, nCVTs were produced through thin-film rehydration and serial extrusion. Doxorubicin (DOX) was subsequently used as a model chemotherapeutic to demonstrate that nCVTs are amendable to similar loading strategies (*e.g.*, active loading) as those already reported for liposomes. Two commercially available liposomal doxorubicin formulations, Myocet® and Caelyx® (EU)/Doxil® (US), are reported to be loaded using citric acid[25] and an ammonium sulfate gradient,[26] respectively. Other gradients, such as transmembrane phosphate gradients, have also been investigated in the literature.[27] Interestingly, a study found that the use of a phosphate gradient produced DOX-loaded liposomes with a pH-dependent drug release profile.[27] Hence, an active loading strategy was adopted for the creation of a pH or an ion gradient across the bilayer membrane of nCVT vesicles for DOX incorporation.

After the successful loading of DOX into nCVTs, the ability of the DOX-loaded nCVTs to effectively deliver the drug was demonstrated through *in vitro* cellular uptake and cytotoxicity studies, and *in vivo* antitumor effect in a mouse xenograft colorectal cancer model. This, in turn, demonstrates the potential of nCVTs as a viable nanocarrier for the targeted delivery of chemotherapeutics in cancer therapy.

Results

Production of CGs and nCVTs

nCVTs were previously reported by our group with the aim of exploiting the simplicity and scalability of synthetic nanoparticles (*i.e.* liposomes) for producing cell-based DDSs.[19] For the cellular component, cell ghosts (CGs) were first produced from U937 monocyte cells by emptying their intracellular contents in a hypotonic solution and resealing the cellular membranes under isotonic conditions (Fig. S1 in the SI). The CGs resuspended in PBS were then used to rehydrate the lipid thin film. The rehydration mixture was extruded through membrane filters of decreasing pore size to produce nanosized nCVTs. Liposomes (LIPO) with an identical lipid composition were produced using the same extrusion steps. The resultant nCVTs and liposomes showed sizes below 200 nm, comparable polydispersity indices (PDIs) (Fig. S2A in the SI), and similar particle concentrations (Fig. S2B in the SI). Having a size below 200 nm enables nCVTs (like other nanocarriers) to still exploit the EPR effect and to be easily sterilized using filtration (through a 0.22 μm sterile filter).

Proof of fusion and protein retention on nCVTs

A FRET assay (Fig. S2C–E in the SI) and immunoprecipitation using streptavidin Dynabeads (Fig. 1) were used to prove the fusion between lipids and cellular components. Both assays confirmed that fusion occurred and that CGs were not simply incorporated inside multilamellar vesicles. In the case of immunoprecipitation, since CGs conjugated with Cy5.5 were used to produce nCVTs, only the biohybrid system exhibited the dual fluorescence signals from NBD (from the lipids) and Cy5.5 (from CGs) (Fig. 1A and B). Successful fusion enabled nCVTs to retain about 30% of the proteins from CGs (Fig. 1C). Further analysis showed that selected protein makers (such as CD9, CD63, and CD11a) were also retained, as nCVTs exhibited a rightward fluorescence shift similar to that of parent cells and CGs (Fig. 1D). Tetraspanins (CD9 and CD63) and lympho-

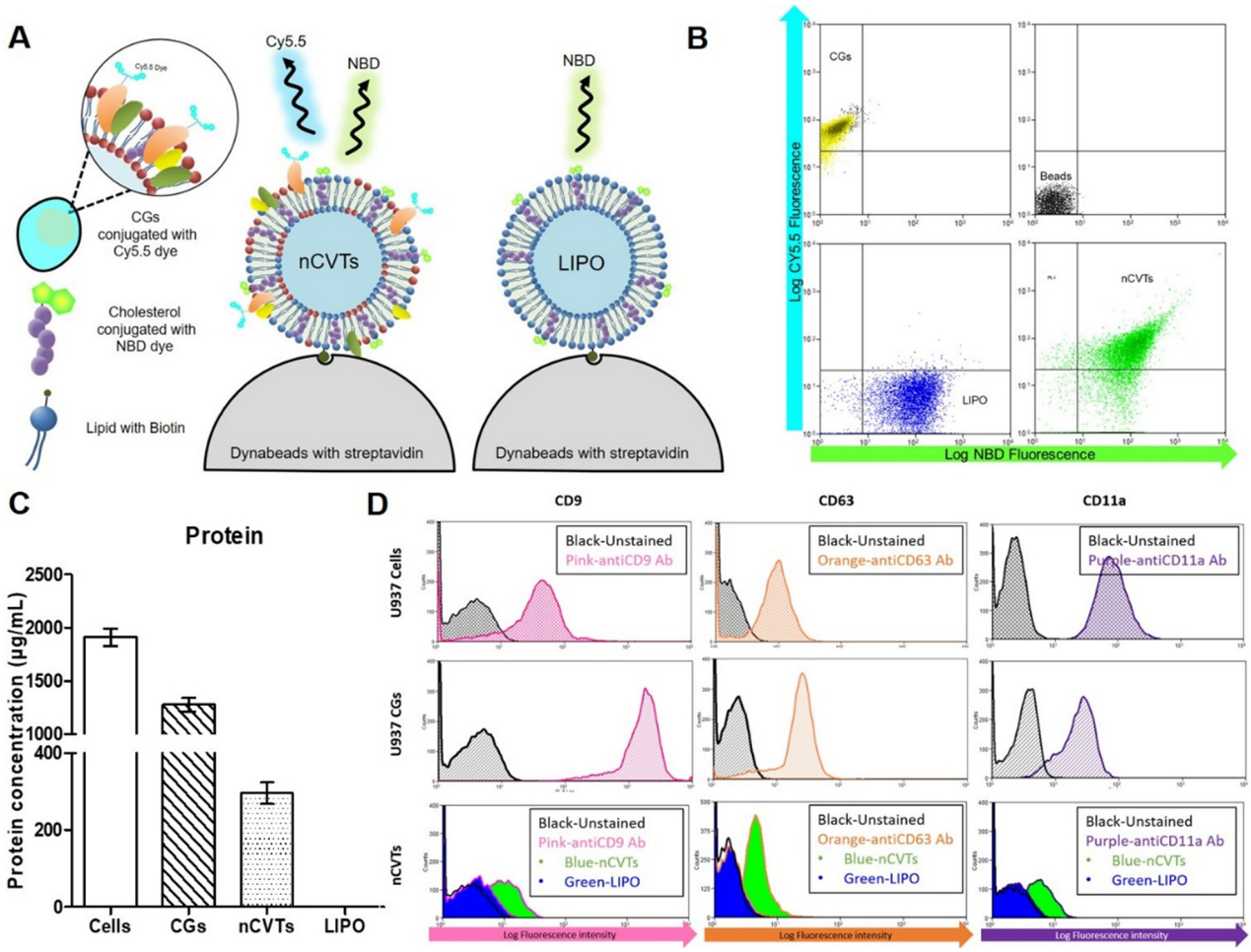

Fig. 1 Proof-of-fusion and presence of protein markers. (A) Schematic of the modified biotin–streptavidin pull-down assay. (B) Flow cytometry dot plots of CGs (top left), beads only (top right), liposomes conjugated onto beads (bottom left) and nCVTs conjugated onto beads (bottom right). nCVTs were made from the fusion of lipids tagged with NBD and CGs conjugated with Cy5.5; thus, the final nCVTs had both NBD and Cy5.5 fluorescence signals. Liposomes, made with lipids and NBD-conjugated cholesterol, had only the NBD signal. (C) Protein retention in nCVTs compared to cells, CGs, and liposomes. (D) Presence of specific markers, namely CD9, CD63, and CD11a (LFA-1), on cells, CGs, and nCVTs, indicating that nCVTs preserved the protein markers from the parent cells.

cyte function-associated antigen-1 (LFA-1 and CD11a) were present on monocytic U937 cells and CGs, and these markers could be transferred to nCVTs after the production process. This further demonstrated the successful fusion and production of nCVTs.

Cellular uptake of nCVTs and liposomes

Fluorescence-labelled vesicles were used to investigate the *in vitro* cellular uptake of nCVTs and liposomes. The vesicles were first normalized based on their fluorescence level before incubation with HeLa, CT26 and HEK293 cells for 1 hour and 4 hours, respectively. From the flow cytometry results shown in Fig. 2A, a significant rightward shift (of green curves), indicating high cellular uptake, was observed in all nCVT-treated samples. The magnitude of nCVT uptake was higher in cancerous cells (*i.e.* HeLa and CT26) than that in non-cancerous cells (*i.e.* HEK293), indicating possible selectivity towards cancerous cells. The uptake of the vesicles was further confirmed using confocal microscopy (Fig. S3). A pronounced Cy5.5 signal (in green), enclosed by CellMask Orange-labelled cell membrane (in red), was observed in nCVT-treated cells after 4 hours of incubation.

We also attempted to investigate the effect of exposure time and temperature on the cellular uptake of nCVTs using HeLa cells. Uptake of both liposomes and nCVTs was found to be time dependent, as demonstrated by increased uptake with prolonged incubation (Fig. 2B). However, the fluorescence of liposomes seemed to plateau (saturation effect) after 2 hours, whereas in nCVTs, the fluorescence continued to increase, thus further suggesting that the presence of cellular components in nCVTs can potentially enhance uptake. To assess the involvement of energy-driven endocytosis in the cellular uptake of these nano-vesicles, incubations were performed at two low temperatures (4 °C and 25 °C). In general, the cellular uptake of both vesicles decreased significantly when low temperatures were used (Fig. 2C). This confirmed that the energy-

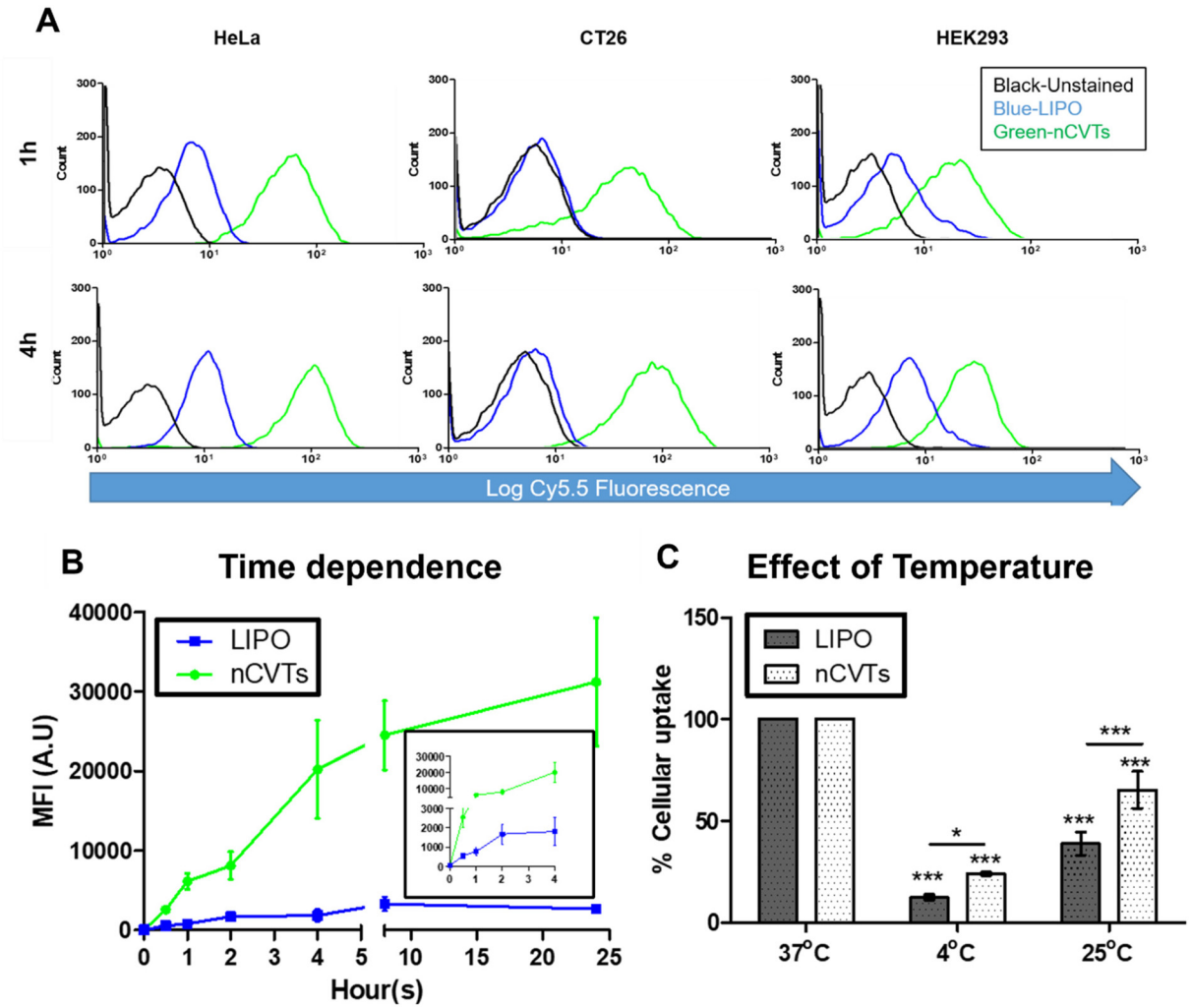

Fig. 2 *In vitro* cellular uptake of nCVTs and liposomes (LIPO). (A) FACS quantitative cellular uptake profile of Cy5.5-labelled nCVTs (green) and Cy5.5-labelled LIPO (blue) in HeLa, CT26 and HEK293 cells after 1 hour and 4 hours of incubation. Cellular uptake of Cy5.5-labelled vesicles at (B) different time points (0.5, 1, 2, 4, 8, and 24 hours) and (C) after 1 hour of incubation at different temperatures (4 °C and 25 °C) compared with the physiological temperature of 37 °C.

driven endocytosis is involved in the internalization of these nano-vesicles, as previously reported.[20]

In order to decipher the mechanism behind the higher uptake of nCVTs *versus* liposomes, we first investigated the involvement of cellular components (*i.e.* membrane proteins) in the homing of nCVTs towards tumor tissues. We hypothesized that the preservation of the structural cues of the parent monocytic cell membranes (*i.e.* U937) may introduce some tumor-tropic capabilities into nCVTs. While tetraspanins (CD9 and CD63) are known proteins involved in targeting and cell adhesion, they usually act as "molecular organizers" by clustering and complexing with relevant molecules to facilitate and stabilize interactions with target cells.[28] On the other hand, the presence of CD11a, as part of LFA-1, on nCVTs may enhance the docking and uptake of the nCVTs by cells overexpressing intercellular adhesion molecules (ICAMs) (*i.e.* cancer cells and tumor-associated endothelial cells). LFA-1 or αLβ2 integrin has been shown to interact with multiple ICAM molecules (especially ICAM-1), which plays a pivotal role in many crucial leukocyte functions, such as adhesion and extravasation.[29,30] Endothelial cells constitutively express low levels of ICAM-1 proteins. However, during tissue damage or in response to inflammatory cytokines such as TNF-α, IL-1, and IFN-γ, the expression of ICAM-1 is significantly increased[30] (Fig. 3A).

To further investigate if the presence of counter receptors (such as LFA-1 or other integrins) for cell adhesion proteins (*i.e.* ICAM-1, VCAM-1, and E-selectin) on nCVTs helps to confer the selective targeting of tumor sites, we conducted an *in vitro* targeting experiment involving TNF-α-treated HUVECs. As depicted in Fig. 3B, without stimulation by inflammatory cytokines, HUVECs did not effectively internalize nCVTs. Interestingly, after stimulation with TNF-α, there was a significant increase in the uptake of nCVTs by the stimulated

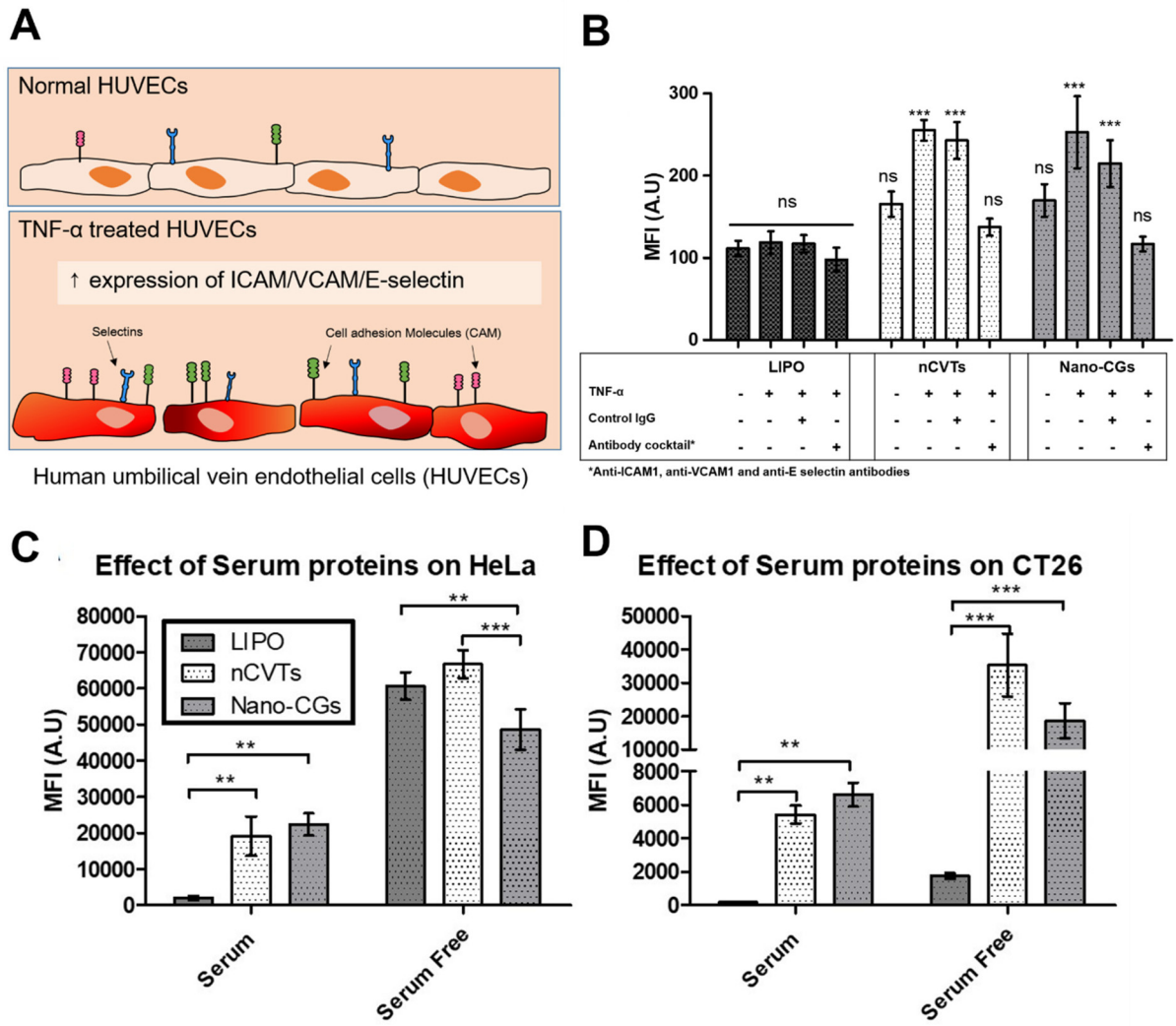

Fig. 3 (A) Schematic of the endothelium at the tumor site. (B) Cellular uptake by TNF-α-treated HUVECs in the absence (–) or presence (+) of a cocktail of neutralizing antibodies (antibodies against ICAM-1, VCAM-1, and E-selectin) or control IgG (isotype control) (n = 3 per group). Cellular uptake of different nanoparticles in the presence or absence of serum (10% FBS) in (C) HeLa and (D) CT26 cells (n = 3/group). ns, not significant, *p < 0.05, **p < 0.01, and ***p < 0.001.

HUVECs. We further validate this selective targeting by blocking cell adhesion proteins on HUVECs by adding a cocktail of neutralizing antibodies against ICAM-1, VCAM-1, and E-selectin. As expected, the treatment with the neutralizing antibodies effectively reduced the uptake of nCVTs, highlighting the involvement of these cell adhesion molecules in the uptake of nCVTs. Importantly, the cellular uptake profile of nCVTs was found to be similar to nano-CGs (CGs extruded into nano-sized vesicles), which suggests that nCVTs acquire their targeting capabilities from their cellular components. On the other hand, liposomes, which did not possess any protein markers and ligands, did not show any significant difference in terms of uptake, regardless of whether HUVECs were stimulated with inflammatory cytokines or subjected to blocking antibodies. These results further illustrate the non-selectivity of liposomes, while the enhanced uptake of nCVTs by TNF-α-treated HUVECs suggests the ability of nCVTs to enhance targeting towards inflammatory tumor sites.

Besides the targeting abilities of DDSs towards diseased areas, another point of consideration for nanocarriers is their interactions with serum proteins and other components in the blood upon intravenous administration. The ungoverned adsorption of these biomolecules onto the nanocarrier results in the formation of a "protein corona".[31] While the composition of the "protein corona" depends on several parameters related to the surface properties of nanoparticles and constituents of the protein environment, the "protein corona" can change the overall surface chemistry of the nanoparticles and thus alter their uptake profile.[32] As illustrated in Fig. 3C and D, the uptake of both nCVTs and liposomes in the presence of serum was lower than in the serum-free controls. However, the decrement was much higher for liposomes than for nCVTs or

nano-CGs, suggesting that nCVTs and nano-CGs are less significantly affected by the presence of serum. In the case of nCVTs, the cellular components on nCVTs may lower the free surface energy[33] and thus, prevent the adsorption of biomolecules/proteins on the surface and reduce the impact on cellular uptake. With the incorporation of cellular components in nCVTs, the surface properties of nCVTs and liposomes could be vastly different, resulting in the formation of a "protein corona" with a different composition.[34] Since the types of deposited proteins can affect the biological interface of nanoparticles and interfere with their uptake (either inhibiting[35] or enhancing[36] it), the cellular component in nCVTs can therefore account for the observed differences in cellular uptake profiles compared with liposomes.

DOX loading of nCVTs and LIPO

We adopted a liposomal loading strategy for DOX (*i.e.* active loading *via* a transmembrane ammonium phosphate gradient) to encapsulate the drug into nCVTs. Specifically, we explored the loading of DOX into nCVTs using the ammonium phosphate buffer. As the unionized form of DOX diffuses across the bilayer membrane, the interior acidic pH protonates DOX. In the presence of other counterions such as phosphate, "salting-out" of DOX occurs, as DOX precipitates inside the vesicles, leading to improved encapsulation (compared with passive loading).

Fig. 4A shows the schematic workflow for DOX loading into nCVTs. Briefly, CGs were first resuspended in ammonium phosphate buffer and then used to rehydrate the lipid film. The rehydration mixture was then extruded. nCVTs in ammonium phosphate buffer were then buffer-exchanged to PBS. A transmembrane ammonium ion gradient was created to generate a pH gradient, thereby facilitating the remote loading of DOX into nCVTs. Uncharged DOX molecules diffused into the core of the vesicles and became polarized. Free un-encapsulated DOX was removed with a Sephadex G50 column. Liposomes (LIPO) were loaded using the same way but without the addition of CGs. The size and PDI of DOX-loaded vesicles were compared with empty vesicles (Fig. 4B). We observed no significant change in size and PDI ($p > 0.05$), which suggests a successful loading of DOX into the vesicles. Using the active loading method, nCVTs and liposomes were able to achieve comparably high encapsulation efficiency of ~80% (Fig. 4C), which indicates that the incorporation of cellular components into the lipid bilayer did not compromise the loading capacity of nCVTs.

Cellular uptake of DOX-loaded vesicles and *in vitro* cytotoxicity

As shown in Fig. 5A, HeLa cells treated with DOX-nCVT showed higher DOX uptake than those treated with DOX-LIPO after 4 hour incubation. The trend was more obvious in CT26 cells, as DOX-nCVT-treated cells showed the highest DOX uptake than other samples. No significant difference in terms of DOX uptake was observed in HEK293 cells across the three formulations. The differences among the various samples were less pronounced than the cellular uptake of Cy5.5-labelled empty samples, possibly because DOX is a small molecule that readily enters all cells. The internalization of DOX was further confirmed using confocal microscopy (Fig. 5B). The DOX intensity (in red) observed across the different samples was similar to the corresponding cellular uptake results shown in Fig. 5A. These images also confirmed that the process of encapsulation into nanoparticles did not alter the ability of DOX to enter cells to function as a DNA intercalator.[7]

The percentage of cells positive for DOX was comparable between DOX-nCVTs and free DOX in HeLa cells. In CT26, cells treated with DOX-nCVTs showed the highest percentage of cells positive for DOX (Fig. 5C). Generally, cells treated with DOX-nCVTs had a higher percentage of cells positive for DOX than cells treated with DOX-LIPO in cancerous cells (*i.e.* HeLa and CT26). Notably, in HEK293 cells, both DOX-LIPO and DOX-nCVTs showed lower percentages of cells positive for DOX compared with free DOX-treated cells, suggesting a potential protective effect of the nanoparticles towards non-cancerous cells.

Finally, DOX-nCVTs showed higher cell killing effects than DOX-LIPO in both HeLa and CT26 at the selected concentrations (Fig. 5D), while no significant difference was observed in HEK293. This is in agreement with the cellular uptake profile, suggesting that the presence of cell membrane components on nCVTs can contribute to an enhanced cellular uptake and subsequently lead to an improved therapeutic effect in cancer cells. Nonetheless, DOX, alone, being able to enter cells freely, displayed very high cytotoxicity. As expected, encapsulated DOX (either in nCVTs or LIPO) would have to cross additional barriers (*e.g.*, lipid bilayer of the vesicles or endosomes) before exerting its cytotoxic effect. Yet, interestingly, DOX-nCVTs at 20 μg mL^{-1} in CT26 were able to achieve comparable effects. Nonetheless, only *in vivo* experiments can explain the added value of encapsulating the drug inside a nano-formulation, which is expected to enhance the bioavailability of the drug at the diseased area and, possibly, decrease the side effects.

In vivo efficacy

With the improvement in cytotoxicity towards cancer cells *in vitro*, we investigated whether nCVTs-DOX could also exhibit an improvement in therapeutic efficacy *in vivo*. We injected CT26 colorectal cancer cells subcutaneously for the tumor to develop. After the tumor was palpable, treatments with free DOX, LIPO-DOX or nCVTs-DOX were performed on alternate days over a period of 2 weeks (Fig. 6A). nCVTs-DOX was able to slow down tumor growth better than LIPO-DOX or free DOX, as evidenced by the smaller tumor harvested on the day of sacrifice on day 25 (Fig. 6B). Throughout the treatment, mice treated with nCVTs-DOX had smaller tumors compared with those receiving saline treatment, free DOX or LIPO-DOX (Fig. 6C). This verifies the higher cytotoxicity of nCVTs-DOX in the treatment of colorectal cancer. Treatment with nCVTs-DOX also demonstrated a significant delay in tumor growth (Fig. 6D) and the highest tumor growth inhibition (TGI) of 59.2% ± 5.6% (Fig. 6E). Tumors harvested from mice treated

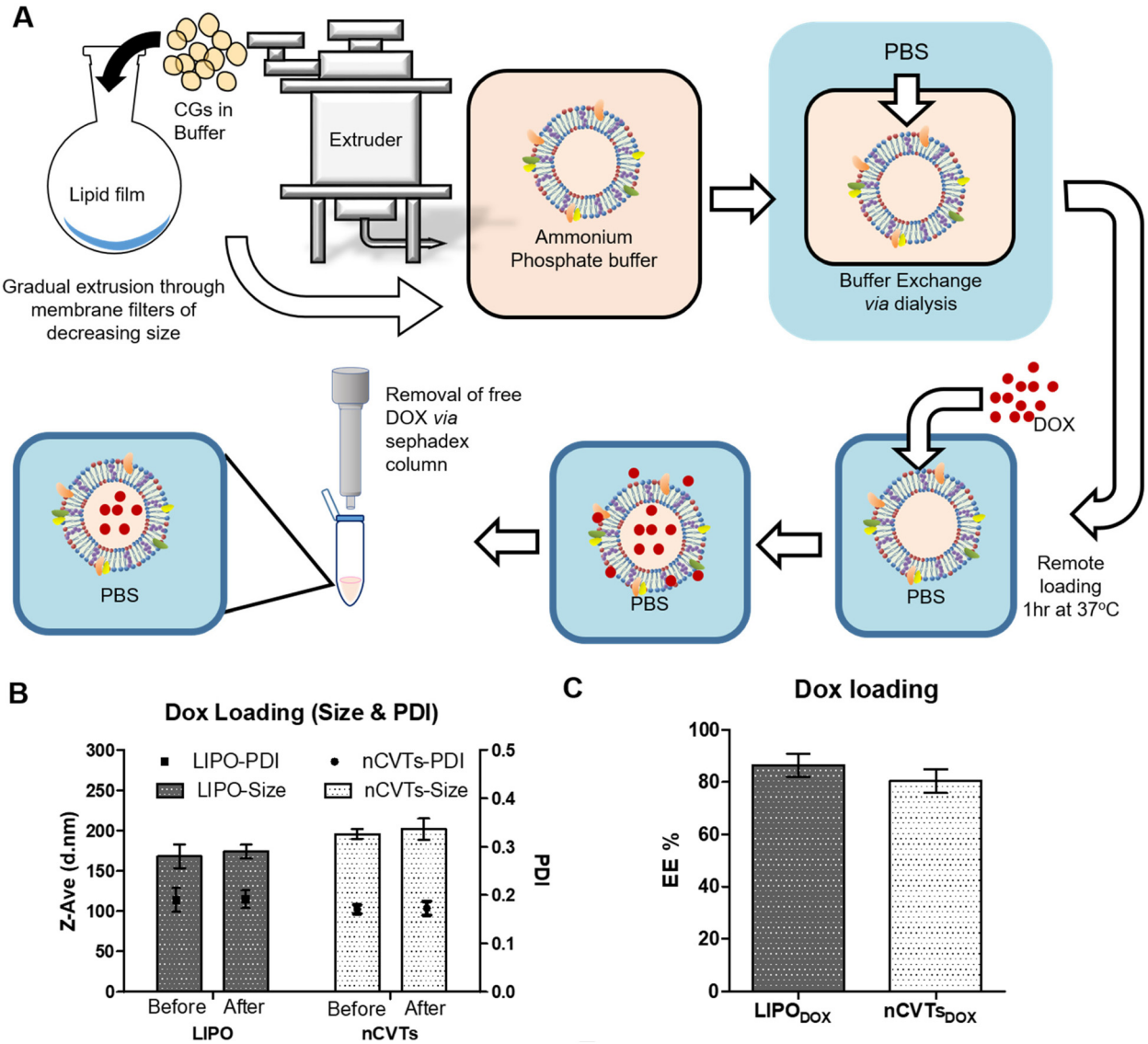

Fig. 4 DOX loading of nCVTs and characterization of DOX-loaded vesicles. (A) Schematic of active loading (*via* an ammonium phosphate gradient) of DOX into nCVTs. CGs resuspended in ammonium phosphate buffer were used to rehydrate the lipid film, followed by extrusion. nCVTs in ammonium phosphate buffer were subsequently buffer-exchanged into PBS. This created a transmembrane ammonium ion gradient, which later translated into a pH gradient to facilitate the remote loading of DOX into nCVTs. Uncharged DOX molecules diffused into the core of the vesicles and became polarized. The un-encapsulated DOX was then separated with a Sephadex G50 column. Liposomes (LIPO) were loaded through a similar protocol but without the addition of CGs. (B) Comparison of size and PDI before and after DOX loading. (C) Encapsulation efficiency of DOX in liposomes and nCVTs.

with nCVTs-DOX also had the lowest tumor dry weight (Fig. 6F). With nCVTs-DOX, doxorubicin could be delivered to the tumor more effectively compared with LIPO-DOX or free DOX. By loading doxorubicin into our biohybrid system, we improved overall therapeutic efficacy. We also collected blood plasma from the mice at the end of the treatment. At a dose of 0.75 mg kg^{-1} doxorubicin, the levels of cardiac troponin I in blood plasma were below the detectable limit of 31.2 pg mL^{-1}. As cardiotoxicity is the main side effect of doxorubicin treatment,[37] our data suggest that it might be possible to further increase the doxorubicin dose or increase the dosing frequency. We expect that our nCVTs-DOX to have a larger therapeutic window compared with free DOX and LIPO-DOX.

Discussion

Cell-derived DDSs have recently gained much attention as potential drug carriers due to their intrinsic targeting abilities. The presence of targeting ligands on the cell membrane gives rise to the preferential uptake and accumulation of drugs by the intended target cells. Furthermore, owing to the natural origin, cell-derived DDSs are considered highly biocompatible. There is also evidence indicating cell-derived DDSs may be

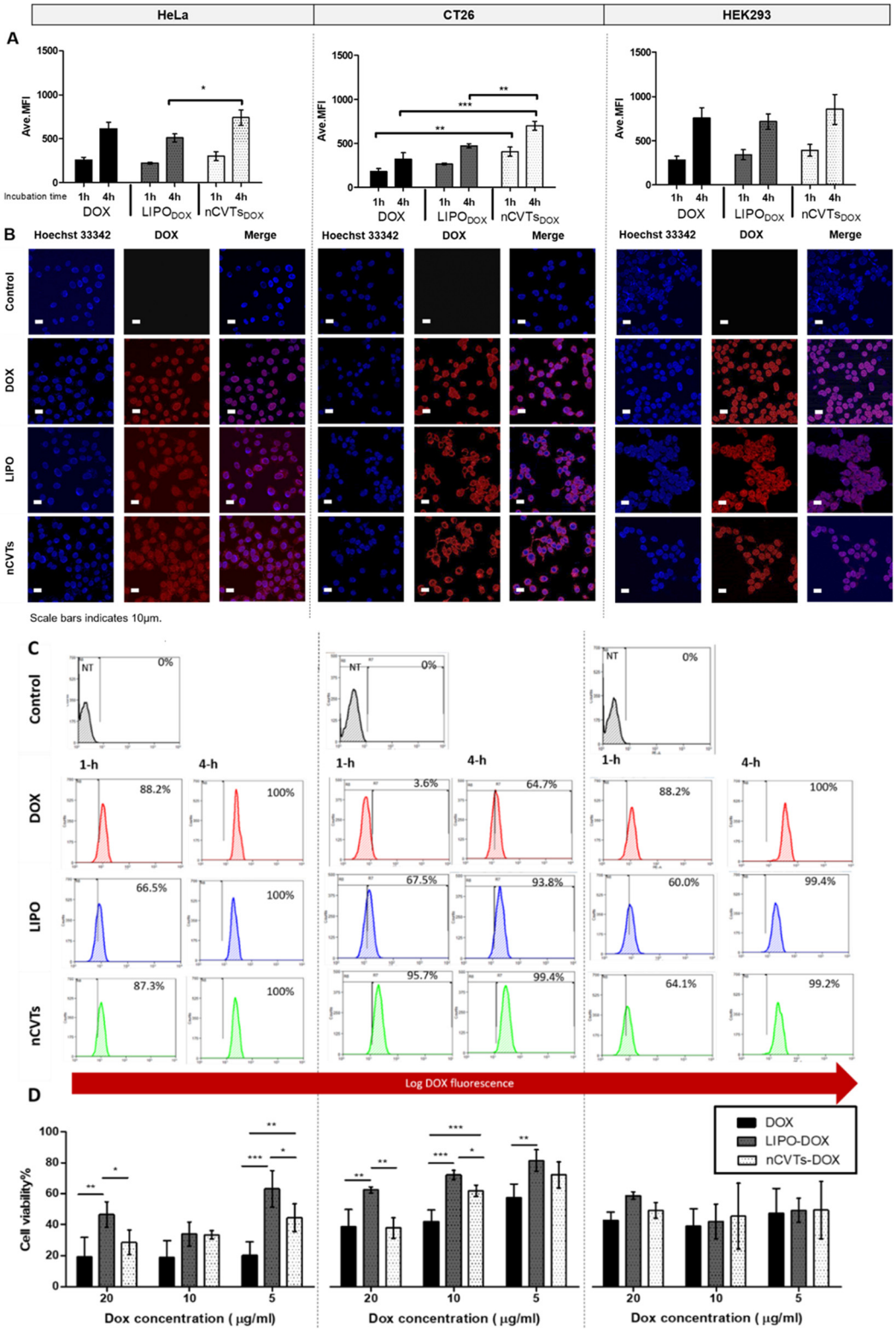

Fig. 5 Cellular uptake and *in vitro* efficiency of DOX-loaded vesicles. (A) Cellular uptake of LIPO-DOX, nCVTs-DOX and free DOX by HeLa, CT26 and HEK293 cells after 1 hour and 4 hour incubation. (B) Confocal microscopy images of DOX-loaded nano-vesicles and free DOX after 4 hour incubation in HeLa, CT26 and HEK293 cells. Scale bar indicates 10 μm. (C) FACS quantification of the percentage of cells that are positive for DOX after 1- and 4 hour incubations. (D) Cell viability of HeLa, CT26 and HEK293 cells after 24 hour incubation with DOX and DOX-loaded vesicles at various concentrations. *$p < 0.05$, **$p < 0.01$, and ***$p < 0.001$.

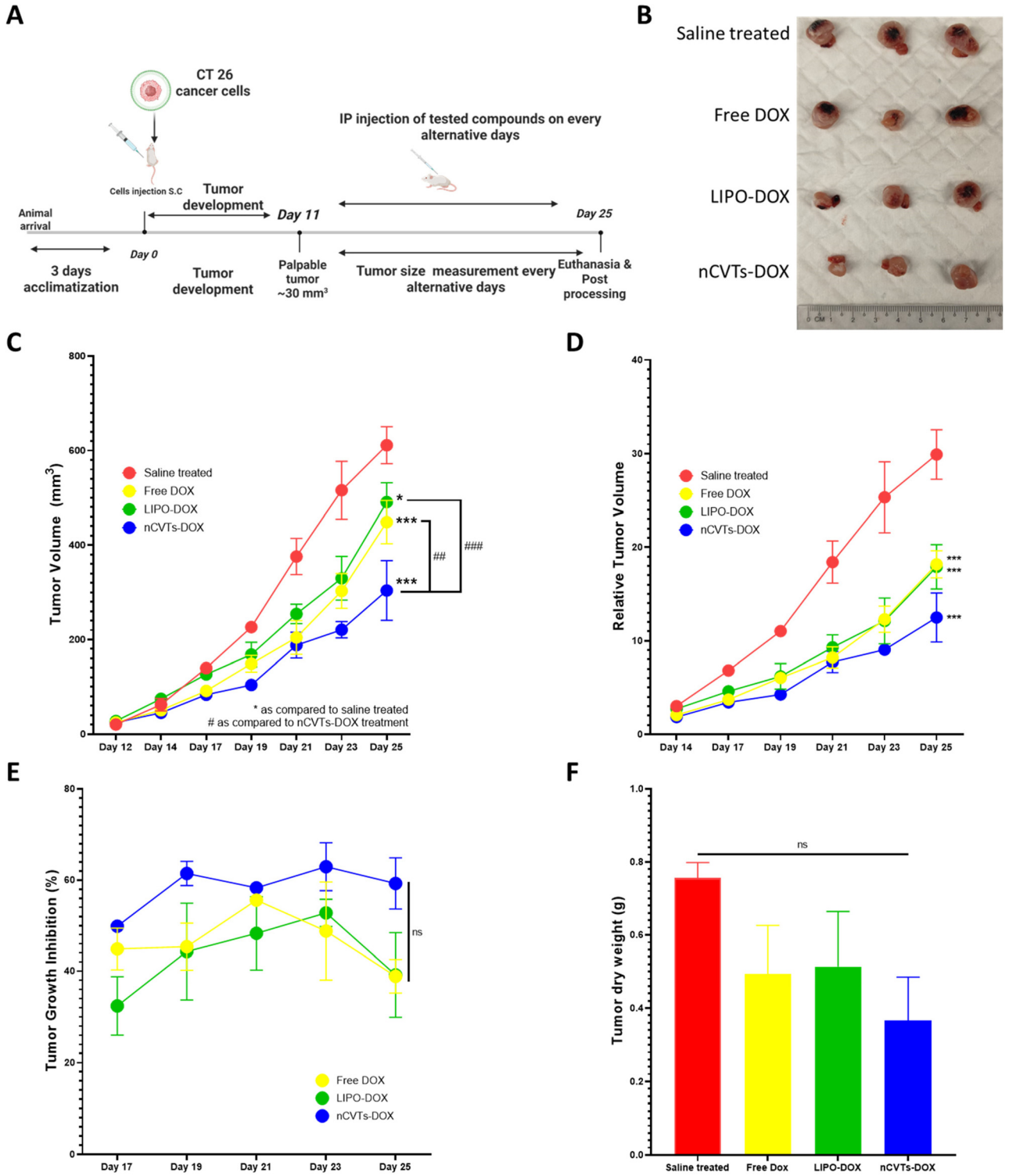

Fig. 6 (A) *In vivo* CT26 colorectal cancer xenograft mouse model. Treatment started on Day 11. (B) Images of tumors harvested after sacrificing mice on Day 25. (C) Tumor volume changes over time with respect to treatment. *$p < 0.05$, ***$p < 0.001$ compared with saline treatment. ##$p < 0.01$, ###$p < 0.001$ compared with nCVTs-DOX treatment. (D) Relative tumor volume changes with respect to its initial tumor volume prior to treatment. ***$p < 0.001$ compared with saline treatment. ##$p < 0.01$, ###$p < 0.001$ compared with nCVTs-DOX treatment. (E) Tumor growth inhibition percentage normalized to the saline-treated group. (F) Dry weight of tumor harvested after sacrifice on day 25. Data are expressed in mean ± SEM ($n = 3$).

immunologically privileged due to the retention of immunomodulatory proteins and lipids.[38,39] Overall, cell-derived DDSs have been explored in various therapeutic areas, including cancer treatment and wound healing.[40,41]

However, the low production and isolation yield of these nano-carriers pose a major limiting factor for their translation in the clinical setting as DDSs.[8] For instance, 0.5 μg of nanovesicles, in terms of protein content, has been reported to be isolated from 10×10^6 cells.[9] Furthermore, incorporating any exogenous molecule (*e.g.*, drugs or other therapeutic agents) into these natural systems is generally more challenging compared with well-established synthetic DDSs like liposomes or micelles. Our group previously developed a novel biohybrid system through the strategic fusion of cellular components and synthetic lipids, with the aim to harness the benefits of liposomes (such as simple and robust production methods and established drug loading protocols) and cell-derived DDSs (such as the preservation of surface cues from their parent cells), which we termed nCVTs. The cellular components used in this study are cell ghosts (CGs) made from emptied U937 monocytes. U937 cells were chosen due to the intrinsic tumor-targeting properties of monocytes, as demonstrated previously.[11] CGs are cells that are devoid of their intracellular content; they are used to minimize variation among batches and reduce excessive protein aggregation (due to cytoplasmic proteins) during the production procedure of nCVTs.[12] Since nCVTs share some structural commonalities with conventional liposomes, we adopted some common liposomal production methods for our nCVTs, namely thin film rehydration and extrusion. Since several commercially available extrusion devices have been established to enable the industrial-scale production of liposomes (*e.g.*, Northern Lipids Inc. (now part of Evonic) has vessel extrusion systems that allow mass production of liposomes in liter-scale[13]), using similar protocols would enable the production of nCVTs in large scale.

As a hybrid system, we successfully demonstrated the fusion of synthetic lipids with cell membrane components in the production of nCVTs. We proved not only the ability of nCVTs to retain proteins (~30% from CGs), but also their capacity to preserve specific cellular markers from the starting CGs. The ability to inherit cellular markers from the original cells indicates the possibility for nCVTs to acquire any cell-specific behaviour or intrinsic targeting ligand, as different cells can be used as starting material to produce nCVTs. Furthermore, besides varying the cellular components to acquire additional functionalities, the lipid components and composition can also be changed. For instance, it is possible to incorporate biotinylated lipids for immunoprecipitation assays or any other ligand-conjugated lipids for additional targeting purposes.

In agreement with our previous work, we demonstrated higher cellular uptake of nCVTs compared with their synthetic counterparts (liposomes) across three different cell lines (*i.e.* HeLa, CT26 and HEK293). This higher cellular uptake of nCVTs can be attributed to the preservation of the cell membrane structure from the parent U937 monocytic cells. Since the CGs used in this study originated from U937, *i.e.* a monocyte cell line known to exhibit intrinsic homing properties towards inflammatory and cancerous sites,[11] it was expected that nCVTs with inherited cell markers from U937 would have the ability to improve targeting towards cancer cells (HeLa and CT26) compared with non-cancerous cells (HEK293). Interestingly, nCVTs did not display obvious saturation in cellular uptake, compared with liposomes, which may suggest better targeting in the tumor environment *in vivo*.

We have previously demonstrated that nCVTs are likely internalized by cells using several concurrent mechanisms, including receptor-mediated pathways.[20] Proteins present on the surface of nCVTs may also play a role in the internalization of nCVTs. The presence of specific protein markers, such as LFA-1, potentially confers tumor tissue specificity to nCVTs. LFA-1 is an integrin that specifically binds to ICAM-1 (CD54), which tends to be overexpressed in many tumor tissues and tumor-associated endothelium.[29,30]

Doxorubicin (DOX) was chosen as the model small-molecule chemotherapeutic, as it is one of the most commonly used drugs in chemotherapeutic regimens and in liposomal research. In this study, DOX was actively loaded into nCVTs *via* an established method adopted for liposomes. A similar encapsulation efficiency of more than 80% was observed for both liposomes and nCVTs. Furthermore, the cellular uptake study and the *in vitro* efficacy assay demonstrated that nCVTs were able to show higher cellular uptake and better cell-killing efficiency compared with liposomes. Although free DOX had the highest cellular uptake and the highest cell-killing efficiency at the measured time-points, it is non-specific and non-selective, which often leads to systemic toxicities *in vivo*, such as cardiotoxicity[14] and myelosuppression.[7] These often-fatal side effects of using DOX were the major reasons behind the development of many liposomal DOX formulations (*e.g.*, Doxil™ and Myocet™).

We demonstrated that DOX-loaded nCVTs (nCVTs-DOX) considerably reduced tumor burden more effectively than both free doxorubicin and liposomal doxorubicin (LIPO-DOX). The surface features of the biohybrid delivery method are likely responsible for the increased antitumor efficacy of nCVTs-DOX. The presence of cellular membrane cues from monocytes, which contributed to enhancing the targeting and uptake of DOX at the tumor site, resulted in an increased antitumor effect of nCVTs-DOX. In addition, although nCVTs were not PEGylated, they were able to circulate *in vivo* long enough to accumulate at the tumor site. This suggests that the incorporation and preservation of surface proteins from CGs can delay immune recognition and reduce nonspecific interactions to a degree comparable to PEGylation. Additionally, we also proved in our previous study that our nCVTs do not elicit any significant immunological response.[20] Overall, our study demonstrates that nCVTs represent a promising, next-generation drug delivery platform that enhances the therapeutic efficacy of DOX by improving targeting specificity, intracellular bioavailability, and drug retention, while also reducing the risk of immunogenicity associated with PEGylated systems.

Taken together, the high encapsulation efficiency, enhanced cellular uptake, and improved *in vitro* and *in vivo* efficiency of nCVTs *versus* the corresponding liposomes suggest that lower doses of nCVTs-DOX (than LIPO-DOX) could be needed to achieve similar pharmacological efficacy. This, in turn, could reduce the risk of adverse reactions through encapsulated chemotherapeutics. The comparative advantages of nCVTs-DOX over LIPO-DOX in terms of targeted cellular uptake and *in vitro* efficiency highlight the potential of nCVTs for the development of the next generation of DDSs.

Experimental section

Materials

Whatman polycarbonate membrane filters (5 μm, 0.4 μm, 0.2 μm, and 0.1 μm) were purchased from GE Healthcare Life Sciences (US). All lipids (Cy5.5-PE (1,2-dioleoyl-*sn-glycero*-3-phosphoethanolamine-*N*-Cyanine5.5), Cy7-PE (1,2-dioleoyl-*sn-glycero*-3-phosphoethanolamine-*N*-Cyanine 7) and DOPC (1,2-dioleoyl-*sn-glycero*-3-phosphocholine)) were purchased from Avanti Polar Lipids (US). Ammonium phosphate was purchased from Merck (US), while doxorubicin hydrochloride (DOX, pharmaceutical grade) and 3-(4,5-dimethylthiazol-2-yl)-2,5-diphenyl-tetrazolium bromide (MTT) were obtained from Sigma-Aldrich (US). A protease inhibitor cocktail was purchased from Abcam (UK).

Cell culture

U937 monocyte cells and CT26 mouse carcinoma cells were kindly provided by Associate Professor Gigi Chiu, National University of Singapore (NUS), and were grown in Roswell Park Memorial Institute medium (RPMI-1640) supplemented with 10% Fetal Bovine Serum (FBS). HEK293 human embryonic kidney cells and HeLa human cervical carcinoma cells were grown in Dulbecco's Modified Eagle Medium (DMEM, high glucose) supplemented with 10% FBS. All cells were maintained in a 5% CO_2 incubator at 37 °C.

"Cell ghost" and nano-CG production

Adopted from the cell-ghost (CG) production protocol from our previous work, U937 cells were harvested at 70% confluency, and 2×10^7 cells were collected by centrifuging at 500*g* for10 minutes; the cells were washed once with phosphate-buffered saline (PBS) to remove residual culture media.[19] The harvested cells were resuspended in 0.25× PBS with 0.06% w/v sucrose (supplemented with 0.5% v/v protease inhibitor cocktail) and incubated on a shaker overnight at room temperature. Subsequently, the cell suspension was centrifuged at 3000*g* for 10 minutes, and the pellet was resuspended in 1× PBS with 0.06% w/v sucrose (supplemented with 0.5% v/v protease inhibitor cocktail). The suspension was incubated on a shaker overnight at room temperature, and the final CGs were kept at 4 °C till further use. Nano-CGs were produced by extruding CGs in a similar fashion to nCVTs but without the lipids.

Production of nCVTs, liposomes, and DOX-loaded formulations

DOPC (2 mg) and cholesterol (7 : 3 molar ratio) were weighed and dissolved in chloroform, and a thin film was formed using rotary evaporation. To label the vesicles, Cy5.5-PE or Cy7-PE (1 mol%) was added during thin-film production. The production of liposomes and nCVTs was adopted from our previously reported protocol.[19] For production of nCVTs, 1×10^7 CGs were first resuspended in PBS before being extruded with a 5 μm polycarbonate membrane filter. The extruded CGs were then used to rehydrate the lipid film. The mixture was sonicated for at least 30 minutes. Then, the dispersion was extruded (jacketed extruder, GenizerTM) at 35 °C through a series of filters with the following diameters: 0.4 μm, 0.2 μm and 0.1 μm. To prepare DOX-loaded nCVTs (DOX-nCVTs), CGs were re-suspended in 250 mM ammonium phosphate (dibasic) buffer instead of PBS and extruded as described above. The final solution of nCVTs was buffer-exchanged into PBS by dialysis using dialysis devices purchased from Thermo Scientific. DOX (200 μg mL^{-1}) was then added in a 1 : 1 v/v ratio. Remote loading was performed at 37 °C for 1 hour. Unencapsulated DOX was then removed using a Sephadex G50 column, which was pre-equilibrated with PBS. Liposomes and DOX-loaded liposomes (DOX-LIPO) were produced using the same way but without the addition of CGs.

Characterizations of vesicles

Dynamic light scattering (DLS; Malvern Zetasizer Nanoseries) was used to determine the size and polydispersity index of nCVTs and liposomes. Standard BCA protein kit was employed to measure the total protein content. Bovine serum albumin (BSA) was used as the standard for protein quantification.

FRET assay and immunoprecipitation using streptavidin Dynabeads were used to prove the fusion between lipids and cellular components. The FRET assay followed a previously reported protocol from our group.[19] Briefly, liposomes and nCVTs were prepared as described earlier with the addition of 1 mol% of NBD- and rhodamine-labelled lipids. Samples were then assayed at 460 nm, and emission spectra from 300 nm to 700 nm were recorded using a microplate reader. For the immunoprecipitation assay, biotinylated nCVTs and liposomes were produced by incorporating biotinylated lipids (1 mol%) and NBD-labelled cholesterol (1 mol%) into the lipid thin film, which was subsequently used to produce the vesicles as previously described.

Particle concentrations were also quantified using a NanoSight NS300 coupled with Nanoparticle Tracking Analysis software (Malvern, UK).

The amount of DOX loaded and the encapsulation efficiency of the loaded vesicles were calculated. Briefly, vesicles were lysed using Triton-X-100 (0.1% v/v) to release encapsulated DOX, and the amount of DOX was determined by a microplate reader at 470/590 nm (Ex/Em) with a DOX calibration curve. The encapsulation efficiency of DOX was calcu-

lated using the following equation:[1]

$$\text{Encapsulation efficiency } (EE) = (\text{encapsulated DOX})/(\text{total DOX}) \times 100\%.$$

In vitro cellular uptake

The Cy5.5-labelled samples and DOX-loaded samples were normalized to their fluorescence intensity and DOX concentrations, respectively, before being added to HeLa, CT26 (cancer cell model) and HEK293 (non-cancer cell model) cells (2×10^5 cells per well). Samples were incubated for 1 hour and 4 hours. After that, cells were washed three times with PBS and trypsinized prior to analysis by flow cytometry (BD LSR Fortessa Flow Cytometry Analyzer). For confocal microscopy, cells were grown on confocal dishes overnight prior to sample addition. After incubation for 4 hours, nuclear stain Hoechst 33342 and/or plasma membrane stain CellMask Orange were added to the cells. The samples were then washed thrice with PBS and fixed with 4% paraformaldehyde before imaging using a confocal microscope (FLUOVIEW FV10i, Olympus).

In vitro cell viability assay

The cytotoxic effects of DOX-loaded vesicles (DOX-nCVTs and DOX-liposomes) and free DOX were evaluated using the standard MTT assay. HeLa, CT26 and HEK293 were seeded in 96-well culture plates at a density of 1×10^4 cells per well and incubated overnight. The DOX-loaded vesicles were normalized to the same DOX concentration prior to being added to the cells. Cells were incubated with the DOX samples for 24 h and 48 h under culture conditions before adding the MTT reagent (0.5 mg mL^{-1}) in serum-free medium. After 1 hour of incubation with MTT, the medium was aspirated, and 100 μL per well of DMSO was added. Absorbance was measured at 570 nm by a spectrophotometer. Cell viability was assessed and compared to cells treated with PBS.

In vitro drug release

The release of DOX was determined using the dialysis method as described in the literature.[6] All samples were normalized to their DOX concentrations before being placed into dialysis tubing (3500 MWCO, Thermo Scientific SnakeSkin). The release study was conducted at 37 °C, whereby 1 mL of each formulation was dialyzed against 2 L of PBS for 60 hours with periodic changes of dialysis buffer. At designated time points, 50 μL of the sample was withdrawn and used for the quantification of DOX using a microplate reader at 470/590 nm (Ex/Em) using a DOX calibration curve. The percentage of DOX release was then calculated and plotted against time.

In vivo experiments

All animal experiments were approved by the Institutional Animal Care and Use Committee (IACUC) at the National University of Singapore (NUS; protocol number R19-0769). Female BALB/c mice (5–6 weeks old) were engrafted subcutaneously with 7.5×10^4 CT26 murine colon cancer cells at the back. Tumors were allowed to develop until palpable (day 11) before starting any treatment.

DOX-normalized samples (0.75 mg kg^{-1} of DOX) or equivalent volume of empty formulations or 100 μL of saline were injected intraperitoneally on alternate days starting from day 12. Tumor width and length were measured using a vernier caliper. After treatment for 12 days (a total of six doses), the mice were sacrificed. Organs were collected, and blood was harvested by cardiac puncture. The blood was centrifuged at 3000*g* for 10 minutes to isolate the serum.

Tumor volume, relative tumor volume and TGI were calculated using the following formulas:

$$\text{Tumor volume} = 1/2 \times (\text{tumor length} \times [\text{tumor width}]^2)$$

$$\text{Relative tumor volume (RTV)} = (\text{tumor volume on measured day})/(\text{tumor volume on Day 0})$$

$$\text{Tumor growth inhibition} = [1 - (\text{RTV of the treated group})/(\text{RTV of the control group})] \times 100\,(\%)$$

Blood serum cardiac troponin I (cTnI) concentration was determined using a Cardiac Troponin I enzyme-linked immunosorbent assay (ELISA) kit purchased from Biomatik (US) (Catalogue Number: EKN49012).

Statistical analysis

One-way analysis of variance (ANOVA) was employed for statistical analysis of the data, followed by Bonferroni *post hoc* tests using GraphPad Prism software (version 5). Differences were considered significant at P-values <0.05.

Conclusions

We demonstrated the development of a hybrid system, nCVTs, which is able to inherit the advantages of both synthetic liposomal and cell-derived DDSs. As such, these nCVTs have advantages, which includes

(1) Simple and robust production;
(2) High encapsulation efficiency;
(3) Intrinsic targeting capability;
(4) Better cellular uptake.

In our study, we chose to load DOX as a model small molecule for cancer therapy. DOX is actively loaded into nCVTs. We demonstrated high encapsulation efficiency of DOX in nCVTs, superior *in vitro* targeted cellular uptake and greater cell-killing efficiency of DOX-nCVTs compared to DOX-LIPO. Moreover, treatment with nCVTs-DOX resulted in an improvement in tumor growth inhibition compared to LIPO-DOX and free DOX, without significant cardiotoxicity.

Taken together, our study highlights the potential of nCVTs as a promising DDS for a highly targeted delivery of chemotherapeutics and to mitigate potential off-target side effects.

Author contributions

YHO: methodology, investigation, data curation, formal analysis, visualization, and writing – original draft. WHC: investigation and formal analysis, visualization, and writing. RPKM: investigation and formal analysis, visualization, and writing. JL: investigation and formal analysis. CKL: investigation and formal analysis. JNNY: investigation and formal analysis. GP: conceptualization, supervision, funding acquisition, and writing – review and editing.

Conflicts of interest

The author Giorgia Pastorin declares interest in an associated patent filing: Goh WJ, Zou S, Pastorin G. 2017. Biomolecular Composites. PCT/SG2018/050376. Filed on 27 July 2018.

Data availability

The data supporting this article have been included as part of the supplementary information (SI). The data include physicochemical characterization of nCVTs, proof-of-fusion experiments and confocal microscopic images of Cy5.5 labelled vesicles. Supplementary information is available. See DOI: **https://doi.org/10.1039/d5nr02316e**.

Acknowledgements

This work was supported by the National University of Singapore (GAP grant numbers A-8001819-00-00 and A-80024435-00-00). The team would also like to thank the Ministry of Education (MOE Tier 2 A-0008496-00-00, Moe Tier 1 grant A-8002543-00-00). Finally, this research is funded by the National Additive Manufacturing Innovation Cluster (NAMIC), a national platform hosted by A*STAR (Award M23N2K0035 or A-8001601-00-00).

HEK293 and HeLa were obtained from ATCC and grown in DMEM supplemented with 10% FBS. All cells were maintained in a 5% CO_2 incubator at 37 °C.

References

1 S. Tran, P.-J. DeGiovanni, B. Piel and P. Rai, Cancer nanomedicine: a review of recent success in drug delivery, *Clin. Transl. Med.*, 2017, **6**(1), e44.
2 T. Stylianopoulos, EPR-effect: utilizing size-dependent nanoparticle delivery to solid tumors, *Ther. Delivery*, 2013, **4**(4), 421–423.
3 K. Ley, C. Laudanna, M. I. Cybulsky and S. Nourshargh, Getting to the site of inflammation: the leukocyte adhesion cascade updated, *Nat. Rev. Immunol.*, 2007, **7**(9), 678–689.
4 H. Jin, J. Su, B. Garmy-Susini, J. Kleeman and J. Varner, Integrin α4β1 Promotes Monocyte Trafficking and Angiogenesis in Tumors, *Cancer Res.*, 2006, **66**(4), 2146–2152.
5 M. J. Mitchell and M. R. King, Leukocytes as carriers for targeted cancer drug delivery, *Expert Opin. Drug Delivery*, 2015, **12**(3), 375–392.
6 G. Ren, X. Zhao, L. Zhang, J. Zhang, A. L'Huillier, W. Ling, A. I. Roberts, A. D. Le, S. Shi, C. Shao and Y. Shi, Inflammatory Cytokine-Induced Intercellular Adhesion Molecule-1 and Vascular Cell Adhesion Molecule-1 in Mesenchymal Stem Cells Are Critical for Immunosuppression, *J. Immunol.*, 2010, **184**(5), 2321–2328.
7 H. Kiefel, S. Bondong, J. Hazin, J. Ridinger, U. Schirmer, S. Riedle and P. Altevogt, L1CAM, *Cell Adhes. Migr.*, 2012, **6**(4), 374–384.
8 C. Rosette, R. B. Roth, P. Oeth, A. Braun, S. Kammerer, J. Ekblom and M. F. Denissenko, Role of ICAM1 in invasion of human breast cancer cells, *Carcinogenesis*, 2005, **26**(5), 943–950.
9 H. Hamidi and J. Ivaska, Every step of the way: integrins in cancer progression and metastasis, *Nat. Rev. Cancer*, 2018, **18**(9), 533–548.
10 A. Benedicto, I. Romayor and B. Arteta, Role of liver ICAM-1 in metastasis (Review), *Oncol. Lett.*, 2017, **14**(4), 3883–3892.
11 Y. Barenholz, Doxil®—The first FDA-approved nano-drug: Lessons learned, *J. Controlled Release*, 2012, **160**(2), 117–134.
12 A. Bunker, A. Magarkar and T. Viitala, Rational design of liposomal drug delivery systems, a review: Combined experimental and computational studies of lipid membranes, liposomes and their PEGylation, *Biochim. Biophys. Acta, Biomembr.*, 2016, **1858**(10), 2334–2352.
13 L. Sercombe, T. Veerati, F. Moheimani, S. Y. Wu, A. K. Sood and S. Hua, Advances and Challenges of Liposome Assisted Drug Delivery, *Front. Pharmacol.*, 2015, 6.
14 Y. Li, M. Kröger and W. K. Liu, Endocytosis of PEGylated nanoparticles accompanied by structural and free energy changes of the grafted polyethylene glycol, *Biomaterials*, 2014, **35**(30), 8467–8478.
15 T. M. D. Els, L. Peter, J. G. O. Wim, S. Gert, L. S. Gerrit, W. M. v. d. M. Jos, H. M. C. Frans and C. B. Otto, Accelerated Blood Clearance and Altered Biodistribution of Repeated Injections of Sterically Stabilized Liposomes, *J. Pharmacol. Exp. Ther.*, 2000, **292**(3), 1071.
16 P. Tiet and J. M. Berlin, Exploiting homing abilities of cell carriers: Targeted delivery of nanoparticles for cancer therapy, *Biochem. Pharmacol.*, 2017, **145**, 18–26.
17 C. E. Olingy, H. Q. Dinh and C. C. Hedrick, Monocyte heterogeneity and functions in cancer, *J. Leukocyte Biol.*, 2019, 1938–3673.
18 T. Lang, Q. Yin and Y. Li, Progress of Cell-Derived Biomimetic Drug Delivery Systems for Cancer Therapy, *Adv. Ther.*, 2018, **1**(7), 1800053.
19 W. J. Goh, S. Zou, B. Czarny and G. Pastorin, nCVTs: a hybrid smart tumour targeting platform, *Nanoscale*, 2018, **10**(15), 6812–6819.

20 Y.-H. Ou, J. Liang, W. H. Chng, R. P. Muthuramalingam, Z. X. Ng, C. K. Lee, Y. R. Neupane, J. N. Yau, S. Zhang, C. K. Lou, C. Huang, J.-W. Wang and G. Pastorin, *Investigations on Cellular Uptake Mechanisms and Immunogenicity Profile of Novel Bio-Hybrid Nanovesicles Pharmaceutics [Online]*, 2022.

21 S. C. Jang, O. Y. Kim, C. M. Yoon, D.-S. Choi, T.-Y. Roh, J. Park, J. Nilsson, J. Lötvall, Y.-K. Kim and Y. S. Gho, Bioinspired Exosome-Mimetic Nanovesicles for Targeted Delivery of Chemotherapeutics to Malignant Tumors, *ACS Nano*, 2013, **7**(9), 7698–7710.

22 S. A.-O. Figenschau, E. Knutsen, I. Urbarova, C. Fenton, B. Elston, M. Perander, E. S. Mortensen and K. A.-O. Fenton, ICAM1 expression is induced by proinflammatory cytokines and associated with TLS formation in aggressive breast cancer subtypes, *Sci. Rep.*, 2018, 2045–2322.

23 J. Y. Oh, H. S. Kim, L. Palanikumar, E. M. Go, B. Jana, S. A. Park, H. Y. Kim, K. Kim, J. K. Seo, S. K. Kwak, C. Kim, S. Kang and J.-H. Ryu, Cloaking nanoparticles with protein corona shield for targeted drug delivery, *Nat. Commun.*, 2018, **9**(1), 4548.

24 L. Rao, Q.-F. Meng, L.-L. Bu, B. Cai, Q. Huang, Z.-J. Sun, W.-F. Zhang, A. Li, S.-S. Guo, W. Liu, T.-H. Wang and X.-Z. Zhao, Erythrocyte Membrane-Coated Upconversion Nanoparticles with Minimal Protein Adsorption for Enhanced Tumor Imaging, *ACS Appl. Mater. Interfaces*, 2017, **9**(3), 2159–2168.

25 C. E. Swenson, W. R. Perkins, P. Roberts and A. S. Janoff, Liposome technology and the development of Myocet™ (liposomal doxorubicin citrate), *Breast*, 2001, **10**, 1–7.

26 E. M. Bolotin, R. Cohen, L. K. Bar, N. Emanuel, S. Ninio, Y. Barenholz and D. D. Lasič, Ammonium Sulfate Gradients for Efficient and Stable Remote Loading of Amphipathic Weak Bases into Liposomes and Ligandoliposomes, *J. Liposome Res.*, 1994, **4**, 455–479.

27 A. Fritze, F. Hens, A. Kimpfler, R. Schubert and R. Peschka-Süss, Remote loading of doxorubicin into liposomes driven by a transmembrane phosphate gradient, *Biochim. Biophys. Acta, Biomembr.*, 2006, **1758**(10), 1633–1640.

28 J. M. Tarrant, L. Robb, A. B. van Spriel and M. D. Wright, Tetraspanins: molecular organisers of the leukocyte surface, *Trends Immunol.*, 2003, **24**(11), 610–617.

29 Y.-M. Hyun, C. T. Lefort and M. Kim, Leukocyte integrins and their ligand interactions, *Immunol. Res.*, 2009, **45**(2), 195–208.

30 B. L. Walling and M. Kim, LFA-1 in T Cell Migration and Differentiation, *Front. Immunol.*, 2018, **9**, 2018.

31 R. Madathiparambil Visalakshan, L. E. González García, M. R. Benzigar, A. Ghazaryan, J. Simon, A. Mierczynska-Vasilev, T. D. Michl, A. Vinu, V. Mailänder, S. Morsbach, K. Landfester and K. Vasilev, The Influence of Nanoparticle Shape on Protein Corona Formation, *Small*, 2020, **16**(25), 2000285.

32 A. Lesniak, F. Fenaroli, M. P. Monopoli, C. Åberg, K. A. Dawson and A. Salvati, Effects of the Presence or Absence of a Protein Corona on Silica Nanoparticle Uptake and Impact on Cells, *ACS Nano*, 2012, **6**(7), 5845–5857.

33 J. V. Jokerst, L. Tatsiana, R. N. Zare and S. S. Gambhir, Nanoparticle PEGylation for Imaging and Therapy, *Nanomedicine*, 2011, **6**(4), 715–728.

34 J. Saikia, M. Yazdimamaghani, S. P. Hadipour Moghaddam and H. Ghandehari, Differential Protein Adsorption and Cellular Uptake of Silica Nanoparticles Based on Size and Porosity, *ACS Appl. Mater. Interfaces*, 2016, **8**(50), 34820–34832.

35 A. Salvati, A. S. Pitek, M. P. Monopoli, K. Prapainop, F. B. Bombelli, D. R. Hristov, P. M. Kelly, C. Åberg, E. Mahon and K. A. Dawson, Transferrin-functionalized nanoparticles lose their targeting capabilities when a biomolecule corona adsorbs on the surface, *Nat. Nanotechnol.*, 2013, **8**(2), 137–143.

36 L. Shen, S. Tenzer, W. Storck, D. Hobernik, V. K. Raker, K. Fischer, S. Decker, A. Dzionek, S. Krauthäuser, M. Diken, A. Nikolaev, J. Maxeiner, P. Schuster, C. Kappel, A. Verschoor, H. Schild, S. Grabbe and M. Bros, Protein corona–mediated targeting of nanocarriers to B cells allows redirection of allergic immune responses, *J. Allergy Clin. Immunol.*, 2018, **142**(5), 1558–1570.

37 P. S. Rawat, A. Jaiswal, A. Khurana, J. S. Bhatti and U. Navik, Doxorubicin-induced cardiotoxicity: An update on the molecular mechanism and novel therapeutic strategies for effective management, *Biomed. Pharmacother.*, 2021, **139**, 111708.

38 S. Kamerkar, V. S. LeBleu, H. Sugimoto, S. Yang, C. F. Ruivo, S. A. Melo, J. J. Lee and R. Kalluri, Exosomes facilitate therapeutic targeting of oncogenic KRAS in pancreatic cancer, *Nature*, 2017, **546**(7659), 498–503.

39 J. Donoso-Quezada, S. Ayala-Mar and J. González-Valdez, The role of lipids in exosome biology and intercellular communication: Function, analytics and applications, *Traffic*, 2021, **22**(7), 204–220.

40 Y. R. Neupane, H. K. Handral, S. A. Alkaff, W. H. Chng, G. Venkatesan, C. Huang, C. K. Lee, J.-W. Wang, G. Sriram, R. A. Dienzo, W. F. Lu, Y. Ali, B. Czarny and G. Pastorin, Cell-derived nanovesicles from mesenchymal stem cells as extracellular vesicle-mimetics in wound healing, *Acta Pharm. Sin. B*, 2023, **13**(5), 1887–1902.

41 W. J. Goh, C. K. Lee, S. Zou, E. C. Woon, B. Czarny and G. Pastorin, Doxorubicin-loaded cell-derived nanovesicles: an alternative targeted approach for anti-tumor therapy, *Int. J. Nanomed.*, 2017, 1178–2013.

